# 41

# THE FREEZE-DRYING PROCESS: THE USE OF MATHEMATICAL MODELING IN PROCESS DESIGN, UNDERSTANDING, AND SCALE-UP

VENKAT KOGANTI AND SUMIT LUTHRA
*Pharmaceutical Development, Pfizer Global Research and Development, Pfizer, Inc., Groton, CT, USA*
MICHAEL J. PIKAL
*University of Connecticut, Storrs, CT, USA*

## 41.1 INTRODUCTION

Freeze-drying, also termed "lyophilization," is a drying process employed to convert solutions of labile materials into solids of sufficient stability for distribution and storage. A typical production scale freeze-dryer consists of a drying "chamber" containing temperature-controlled shelves that is connected to a "condenser" chamber via a large valve. The condenser chamber houses a series of plates or coils capable of being maintained at very low temperature (i.e., less than −50°C). One or more vacuum pumps in series are connected to the condenser chamber to achieve pressures in the range of 0.03–0.3 Torr in the entire system during operation. A commercial freeze-dryer may have 10–20 shelves with a total load on the order of 50,000 10 cc vials. The objective in a freeze-drying process is to convert most of the water into ice in the "freezing stage," remove the ice by direct sublimation in the "primary drying stage," and finally remove most of the unfrozen water in the "secondary drying" stage by desorption. The water removed from the product is reconverted into ice by the condenser.

In a typical freeze-drying process, an aqueous solution containing the drug and various formulation aids, or "excipients," is filled into glass vials, and the vials are loaded onto the temperature-controlled shelves. The shelf temperature is reduced, typically in several stages, to a temperature in the vicinity of −40°C, thereby converting nearly all of the water into ice. Some excipients, such as buffer salts and mannitol, may partially crystallize during freezing, but most "drugs," particularly proteins, remain amorphous. The drug and excipients are typically converted into an amorphous glass also containing large amounts of unfrozen water (15–30%) dissolved in the solid (i.e., glassy) amorphous phase. Thus, most of the desiccation actually occurs during the freezing stage of the freeze-drying process. After all water and solutes have been converted into solids, the entire system is evacuated by the vacuum pumps to the desired control pressure, the shelf temperature is increased to supply energy for sublimation, and primary drying begins. Due to the large heat flow required during primary drying, the product temperature runs much colder than the shelf temperature. The removal of ice crystals by sublimation creates an open network of "pores" that allows pathways for escape of water vapor out of the product. The ice–vapor boundary (i.e., the boundary between frozen and "dried" regions) generally moves from the top of the product toward the bottom of the vial in roughly planar fashion as primary drying proceeds. Primary drying is normally the longest part of the freeze-drying process. Primary drying times on the order of days are not uncommon, and in rare cases, weeks may be required for a combination of poor formulation and suboptimal process design. While some secondary drying does occur during primary drying (i.e., desorption of water from the amorphous phase occurs to a limited extent once the

*Chemical Engineering in the Pharmaceutical Industry: R&D to Manufacturing* Edited by David J. am Ende

ice is removed from that region), the start of secondary drying is normally defined, in an operational sense, as the end of primary drying (i.e., when ice is removed). Of course, since not all vials behave identically, some vials enter secondary drying while other vials are in the last stages of primary drying. When the judgment is made that all vials are devoid of ice, the shelf temperature is typically increased to provide the higher product temperature required for efficient removal of the unfrozen water. The final stages of secondary drying are normally carried out at shelf temperatures in the range of 25–50°C for several hours. Here, since the demand for heat is low, the shelf temperature and the product temperature are nearly identical.

Since freeze-drying plants are very expensive and process times are often long, a freeze-dried dosage form is relatively expensive to produce. Indeed, because of both cost and ease of use, a "ready-to-use" solution is the preferred option for a parenteral dosage form, particularly if the solution can withstand terminal heat sterilization. However, most parenteral drugs undergo excessive degradation during terminal sterilization. Even if sterility requirements may be satisfactorily met without terminal sterilization (i.e., sterile processing), many drugs do not have sufficient stability in the solution state to allow the long-term storage required for pharmaceutical products. Certainly, terminal sterilization is not an option for a protein product. Indeed, many proteins are insufficiently stable in aqueous solution, even when refrigerated, to allow storage for more than a few months without suffering significant degradation. Of course, some proteins are quite stable in aqueous solution, insulin being the classic example of a "solution stable" protein product [1]. When an aqueous solution does not have sufficient stability, the product must be produced in solid form. At least for small molecules, stability normally increases in the order: solution $\ll$ glassy solid $<$ crystalline solid [2–4], likely a result of restricted motion in solids with the high degree of order in the crystalline solid limiting reactivity even further. It should also be noted that the enhanced stability upon crystallization of a solid noted for small molecules may not extend to proteins. Although a direct experimental comparison is limited to one example, that of insulin, crystalline insulin is actually significantly less stable than amorphous freeze-dried insulin [5]. Since pharmaceutical proteins cannot generally be produced on a commercial scale by crystallization, a glassy solid is usually the only solid-state option.

Freeze-drying [6–9] and spray drying [10–12] are drying methodologies in common use in the pharmaceutical industry that are suitable for the production of glassy solids. Freeze-drying is basically a low temperature process. In general, a protein formulation can be dried to on the order of 1% water or less without any of the product exceeding 30°C. Thus, conventional wisdom states that freeze-drying is less likely to cause thermal degradation than a "high temperature" process, such as spray drying. However, it must be noted that due to self cooling as the water evaporates, the product temperature in a spray drying process is far less than the input air temperature, and residence times in the dryer are very short. Indeed, it has been shown that, suitably formulated, stable protein glasses may be produced by direct evaporative drying (i.e., drying without freezing) [13, 14]. Such direct evaporative drying process may involve spray drying or alternate new technologies [15]. While some of the factual material in reference 14 has been challenged [16], it must be admitted that freeze-drying is not the only process by which proteins solutions may be successfully converted into "stable" glasses.

Historically, freeze-drying is the method of choice for products intended for parenteral administration. Sterility and relative freedom from particulates are critical quality attributes for parenterals. Largely because the solution is sterile filtered immediately before filling into the final container, and further processing is relatively free of exposure to humans, a freeze-drying process maintains sterility and "particle free" characteristics of the product much easier than processes that must deal with dry powder handling issues, such as dry powder filling of a spray dried or bulk crystallized powder. Indeed, with modern robotics automatic loading systems [17], humans can be removed from the sterile processing area entirely, at least in principle. Furthermore, since the vials are sealed in the freeze-dryer, moisture and headspace gas can easily be controlled, an important advantage for products whose storage stability is adversely affected by residual moisture and/or oxygen. Since the critical heat and mass transfer characteristics for freeze-drying are nearly the same at the laboratory scale as in full production, resolution of scale-up problems tends to be easier for a freeze-drying process than for spray drying, at least in our experience. Also, development of a freeze-dried product requires less material for formulation and process development, a particularly important factor early in a project.

While freeze-drying has a long history in the pharmaceutical industry as a technique for stabilization of labile drugs, including proteins, many proteins suffer irreversible change, or degradation, during the freeze-drying process [18–22]. Even when the labile drug survives the freeze-drying process without degradation, the resulting product is rarely found perfectly stable during long-term storage, particularly when analytical techniques with a sensitivity to detect low levels of degradation (i.e., $\approx$0.1%) are employed. Both small molecules [2–4, 23] and proteins [24–27] show degradation during storage of the freeze-dried glass. In many cases, instability is serious enough to require refrigerated storage [24, 25, 28].

Stability problems are most often addressed by a combination of formulation optimization and attention to process control. Lyoprotectants are added to stabilize the protein during the freeze-drying process as well as to provide storage stability, and the level and type of buffer is optimized. Optimization of the freezing process may be critical, control of product temperature during drying is critical for products

that tend to suffer cake "collapse" during primary drying, and control of residual moisture is nearly always critical for storage stability. Formulation and process are interrelated in that the process design depends on formulation, and process variations, particularly freezing variations, can change the physical state of the formulation. A bad formulation can be nearly impossible to freeze-dry, and even with a well designed formulation, a poorly designed process may require more than a week to produce material of suboptimal quality. While blind empiricism may, in time, yield an acceptable formulation and process, an appreciation for the materials science of amorphous systems and some understanding of heat and mass transfer relevant to freeze-drying are needed for efficient development of freeze-dried pharmaceuticals. Obviously, one also requires at least a phenomenological understanding of the major degradation pathways specific to the protein under consideration.

Once a suitable formulation and process are developed in the laboratory, hopefully at least close to optimized, the laboratory process needs to be transferred to manufacturing. While freeze-drying is, in many ways, a relatively easy process to scale-up since the volume and the nature of the primary container system is independent of scale (i.e., the same fill volume and vial in both laboratory and manufacturing), there do exist a number of differences between laboratory and manufacturing. First, the timescales are often far different for some stages of the process, the most notable being the time required for loading a manufacturing dryer being much longer than the corresponding time in the laboratory. Thus, particularly if the relative humidity in the vicinity of the freeze-dryer is high, one may experience condensation on the shelves during loading a production dryer but not during the corresponding operation in the laboratory. Such condensation may cause freezing variations that have consequences for the drying process as well. In addition, it is often possible to change shelf temperature very rapidly in the laboratory, but due to greater thermal mass in the manufacturing environment, the production dryer may be unable to match the laboratory dryer's performance. Secondly, there may exist heat and mass transfer differences between the laboratory dryer and the production dryer that require a slightly different shelf temperature profile with time for manufacturing than was used for the laboratory process [29]. Since the objective is to maintain the same product temperature history during the process in manufacturing that was validated in the laboratory, the shelf temperature versus time program in manufacturing may well be different than found optimal for the laboratory [29]. In addition, the maximum heat and mass transfer that the dryer can handle without loosing control varies with the dryer design, and one may find that a process that runs very well in the laboratory dryer may overload the manufacturing dryer and cause loss of chamber pressure control [29]. However, the most important and most troublesome scale-up issue is often the difference in freezing behavior that one experiences in the Class 100 "clean" environment of the production operation relative to the relatively high particulate content in the laboratory air. Thus, typically [30] supercooling is greater in manufacturing than in the laboratory, and since the size of the ice crystals (and resulting pores in the dry cake) decreases with increasing degree of supercooling, the laboratory produces larger ice crystals, larger pores, and less resistance to vapor transport. The net result is that the primary drying time is shorter in the laboratory than in manufacturing, and the product temperature runs colder in the laboratory than in manufacturing. The effect can be significant, with primary drying running from 10% to 30% longer in manufacturing [30–32]. Thus, the material being freeze-dried in the laboratory is typically not representative of the material being dried in production, simply because the freezing behavior is different. Frequently, the process is arbitrarily adjusted in an attempt to compensate for this anticipated difference. That is, the duration of primary drying is extended so that one may be reasonably confident that in the production batch all vials are devoid of ice when the shelf temperature is increased to facilitate secondary drying. However, one is never sure of how much extension is necessary, so there are better solutions to the problem, as discussed in more detail later in this chapter.

Freeze-drying is one of the few unit operations where the underlying physics is relatively well understood, and the theoretical models are not mostly empirical. Thus, modeling can be used very effectively for process design and scale-up using simple steady-state models [33] or more elaborate non-steady-state models that address both sublimation and desorption drying [34]. Use of the theoretical models, with appropriate input data to define heat and mass transfer parameters, allows greater insight into the impact of changes in operating conditions on product quality and brings much greater efficiency into robustness testing than possible with the empirical testing characteristic of pure statistical approaches.

This chapter begins with a detailed discussion of the freezing process, with suggestions for circumventing the problems arising from freezing differences between laboratory and manufacturing, and includes a brief discussion of the few attempts to model freezing behavior. We then continue with a discussion of drying behavior, which includes a detailed discussion of the utility of the various theoretical models that can be effectively utilized in process design and scale-up. We conclude with a brief discussion of modeling vapor flow within the freeze-dryer, a topic of importance but one that has received little attention in the literature.

## 41.2 FREEZING PROCESSES

Freezing is the first step in the lyophilization process where most of the water is separated from the solute as ice crystals.

It is also a very important step as the structure of the frozen matrix governs the rate of sublimation and desorption. Figure 41.1 shows the shelf and product temperature profiles of product frozen in vials on a laboratory-scale shelf freeze-dryer. The data shown are for 5% w/w sucrose solution. During the cooling step, the solution remains liquid well below the equilibrium freezing temperature (−13°C for the example shown in Figure 41.1). Ice nucleation occurs in the supercooled liquid in a stochastic manner and proceeds rapidly. Nucleation is quickly followed by crystal growth. Ice nucleation can occur by two mechanisms: homogeneous or heterogeneous. Homogeneous nucleation is defined as aggregation of pure material (in this case water, which undergoes homogenous nucleation at −40°C) [35]. Heterogeneous nucleation, on the other hand, occurs when aggregates form on foreign solids such as dirt and container wall. Homogeneous ice nucleation does not occur in pharmaceutical freeze-drying operations due to inevitable presence of foreign solids. The foreign surface acts as a catalyst thus reducing the surface free energy for formation of the nuclei. This lowering of free energy means that degree of supercooling is less as compared to homogeneous nucleation. The size of the ice crystals is dependent on the nucleation and growth rate, which are both governed by the degree of supercooling. A higher nucleation rate would result in smaller ice crystals and vice versa. The stochastic nature of nucleation would mean different degrees of supercooling and thus differences in ice crystal size and distribution across the batch and significant differences between batches, particularly when laboratory and production batches are compared [30]. In general, it is desirable to have larger ice crystals and narrow size distribution. Therefore, control over degree of supercooling is desirable. However, to date, the methods to control ice nucleation are only in the experimental stage and have not yet been applied in commercial setting. These issues are discussed in more detail later.

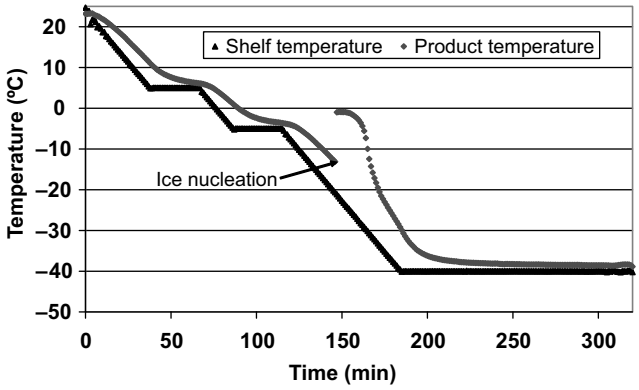


**FIGURE 41.1** Typical shelf and product temperature profile during freezing for a formulation containing amorphous solute. The data are for 5% w/w sucrose solution lyophilized in a laboratory-scale freeze-dryer. The product temperature profile is recorded with a thermocouple located at the bottom center of the vial. The product temperature profile shows significant supercooling before ice nucleation. Ice nucleation causes an increase in product temperature up to approximately the equilibrium melting point. The product temperature stays high as ice crystallization proceeds and it eventually starts to drop and follow the shelf temperature.

### 41.2.1 Cooling Rate

In a typical freezing process the only variable that is under direct control is the cooling rate of the shelf fluid. Further, the range of cooling rates achievable is not particularly large. At most, the samples can be cooled at ≈2°C/min. It has been noted that a cooling rate of 1°C/min is generally optimal as it provides moderate supercooling and reasonably fast freezing rate [36].

### 41.2.2 Solute Concentration and Phase Changes

When liquid water is removed as ice crystals as freezing proceeds, the solutes (active pharmaceutical ingredient (API) and excipients) are concentrated in the unfrozen region between the ice crystals. The concentration continues until the solute crystallizes or converts into an amorphous glassy system. The physical nature of the solutes and their properties has a profound impact on the rest of the process and merits further discussion. Upon completion of freezing, the solute matrix may be completely amorphous, or crystalline, or a mixture of amorphous and crystalline phases. The importance of this matrix is in the mechanical structure it provides for efficient drying and formation of an elegant product. However, to maintain this solid matrix it is important that the product temperature during primary drying should not increase above a critical temperature known as the collapse temperature. In completely amorphous matrices, the collapse temperature ($T_c$) is related to the glass transition temperature of the frozen concentrate ($T_g'$) and is generally about 2°C higher than $T_g'$ [37]. In a completely crystalline matrix, $T_c$ is equal to the temperature of the eutectic melt ($T_{eu}$)[1]. The relationship in a mixed amorphous and crystalline system is governed by the relative ratio of amorphous and crystalline phase [38]. In most cases, mixed systems are dominated by the crystalline phase by design so the effective collapse temperature is close to the eutectic melt even though the collapse temperature (and $T_g'$) of the amorphous phase may be much lower. These crystalline phases designed into the product are called bulking agents and are added to provide mechanical strength and/or raise the effective collapse temperature. Mannitol is the most commonly used bulking agent.

[1] A rigorous definition of "eutectic melting" in ternary systems requires all the components to exist in the crystalline state. This is not the case in the majority of pharmaceutical systems for freeze-drying. However, we have retained the term "eutectic" to describe solute + ice melting, as is the practice in the pharmaceutical community.

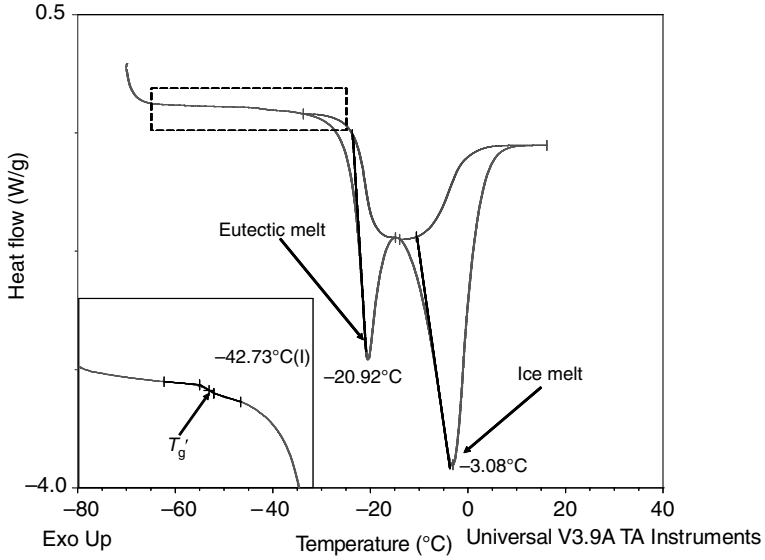


**FIGURE 41.2** Thermogram of a frozen solution containing amorphous and crytalline solutes obtained by differential scanning calorimetry. The heating curve shown displays the glass transition temperature of the amorphous frozen concentrate ($T_g'$), Eutectic melt of crystalline component ($T_{eu}$) and the ice melt event. The data show that there is approximately 20°C window between $T_g'$ and $T_{eu}$ where annealing could be carried out.

Figure 41.2 shows the thermogram for a frozen solution containing amorphous and crystalline solutes. The heating curve shows the presence of $T_g'$ and $T_{eu}$ followed by the ice melting endotherm.

### 41.2.3 Annealing

Annealing is carried out by holding samples isothermal above the $T_g'$ for few hours. It is relatively common to employ an annealing step to facilitate solute crystallization of API or bulking agents [39]. Figure 41.3 shows the shelf and product temperature profile for a solution containing solute that crystallized during freezing. The data shown are for 5% w/w mannitol solution freeze-dried on a laboratory scale freeze-dryer. The shelf temperature profile includes an annealing step at −20°C in this case. A distinct feature of the product temperature profile in this case is the appearance of bumps during the annealing step. These bumps are likely a result of heat released due to crystallization of solute and water during annealing. However, ice nucleation in adjacent vials could be another explanation for the observed bumps. Annealing is also currently the only commercially viable method to modify ice morphology. Annealing is believed to result in increased mean crystal size and narrower distribution due to Ostwald ripening [40]. When the frozen matrix is heated above $T_g'$, the ice crystals below a critical size decrease in size and effectively "melt," and those larger than the critical size grow in a diffusion-dependent manner. The increase in mean size and narrower distribution are both advantageous as larger ice crystals means larger pores for water vapor to escape during primary drying and narrowing of size distribution results in batch homogeneity. The changes in primary drying time that have been reported are significant, such as a 3.5-fold increase in primary drying rate reported in one study [4]. This increase in primary drying rate is correlated with a decrease in mass flow resistance of the dry layer, as reported in another study [41]. However, there have been reported cases (and unpublished experience of the authors) where annealing has not led to a decrease in

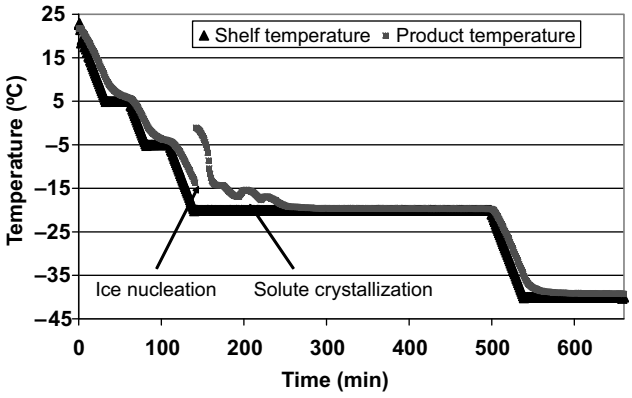


**FIGURE 41.3** Typical shelf and product temperature profile for a formulation containing a crystallizable solute. The data are for 5% mannitol w/w solution freeze-dried in a laboratory-scale freeze-dryer. The shelf temperature profile incorporates an annealing step at -20°C. In addition to the ice nucleation event observed in Figure 41.1 thermal event related potentially to solute crystallization are apparent in the product temperature profile.

mass flow resistance or increase in primary drying rate [42]. There are other reasons why annealing may not be suitable in all cases. The increase in the size of ice crystals will reduce the surface area, which decreases desorption rate during secondary drying and/or prolong reconstitution time. The residual water content of the dried product may therefore be higher [43]. Annealing may also promote phase separation resulting in unintended crystallization of a solute such as a buffer, which would produce a large pH shift, or phase separation within the amorphous phase [44]. Such phase separations may adversely affect the in-process or storage stability of lyophilized protein products where lyoprotectants are used to improve physical and chemical stability and are required to be in the same phase as the protein to impart the stabilization effect. Thus, the benefit of annealing in reducing primary drying time and improving batch homogeneity may be offset by stability problems that might arise from phase separation and in some cases, the additional time required for annealing and secondary drying may negate the reduction in primary drying time. Certainly, optimization of the annealing step is required to achieve the greatest benefit.

### 41.2.4 Methods to Control Ice Nucleation

There are other methods that are currently under development to control the ice nucleation temperature. Ice fog technology is based on introducing cold nitrogen gas in the drying chamber to create an ice fog at the desired temperature of nucleation [45]. The concept was further [32] developed to evaluate the impact of nucleation temperature on mass flow resistance of the dry layer and primary drying time. An empirical direct correlation between specific surface area and mass flow resistance was also established. It was shown that a lower degree of supercooling, that is, nucleation occurring at a higher temperature led to smaller specific surface area and faster primary drying. It was noted that the technique required more development to be a viable method for nucleation control. The use of ultrasound to induce ice nucleation has also been published [46]. Ice nucleation is thought to occur through bubble cavitation. A direct correlation between ice nucleation temperature and sublimation rate during primary drying was observed. Induction of ice nucleation through electric high-voltage pulses has also been published and has been shown to impact primary drying rate [47, 48]. The method known as electrofreezing was only successful for solutions containing nonionic species. None of these methods has actually been applied to a commercial process. Commercial application may require retrofitting of existing units, which would be expensive in the least but may also be impractical in other cases. Nonetheless, these methods do demonstrate that that control of ice nucleation temperature has great potential benefit. An option that would not require any changes to the existing equipment would be preferable, such as induction of freezing by vacuum. A vacuum freezing method to induce top–down freezing arising from evaporative cooling has been published [49, 50]. The method would require further development to address concerns with secondary drying kinetics and residual water content similar to annealing. In addition, top–down freezing may increase the chances of vial breakage and the technique needs to be carefully controlled to avoid boiling and the resulting splattering of the solution.

### 41.2.5 Modeling of the Freezing Process

Freezing processes relevant to lyophilization, that is, in vials has been discussed in the literature [51]. For the purpose of modeling, the process has been divided into two parts: cooling and freezing. The cooling step has been modeled using Fourier's second law and is straightforward as the input parameters density, heat capacity, cooling rate, and thermal conductivity of the solution can be easily determined from published literature and experimentation. Modeling of the freezing step becomes more complicated as one would expect because the theories of nucleation and crystallization are less well defined than simple heat transfer. Also, the terms involving phase changes introduce additional parameters that at best are difficult to estimate or measure. Nonetheless, this approach was used to estimate mean ice crystal size and mass flow resistance of the dry layer. It is clear that modeling the freezing step is not as advanced as the drying steps and is not at a level where a scientist would determine the input parameters in the laboratory and plug the values into a simple model that produces useful quantitative results. However, the published data do confirm some general concepts that nucleation temperature and cooling rate both impact the mean ice crystal size and distribution and that increasing the nucleation temperature and lowering the cooling rate result in larger ice crystals, thus lower mass flow resistance of the dry layer. Additional progress in modeling the freezing process is needed so that the impact of process variations, for example, annealing, on the mean ice crystal size and distribution could be accessed and the mass flow resistance parameter for modeling the drying process could readily be obtained.

### 41.2.6 Scale-Up Issues

The manufacturing of clinical or commercial pharmaceutical products is conducted in sterile, particulate free, Class 100 areas whereas lyophilization cycle development is generally conducted in laboratories that are not at all "particle free." The particulate load, that is, heterogeneous nucleation sites, thus vary when scaling up from laboratory to clinical or commercial site. This means that the degree of supercooling in a production environment would be greater, leading to smaller ice crystals and higher resistance to mass flow through the dried layer. Therefore, primary drying parameters developed in the laboratory would generally lead

to higher product temperature and longer drying time in the production environment [30].

### 41.2.7 Rational Freezing Process Development

A development scientist should take (essentially) the following approach to develop a rational freezing process.

1. *Selection of Cooling Rate*: The impact of cooling rate parameter has been discussed previously in this chapter. In summary, a cooling rate between 0.5 and 1°C/min would generally lead to moderate supercooling, which is uniform intravial and intervial, while providing a sufficiently fast freezing rate to avoid phase separation.
2. *Selection of Final Freezing Temperature and Time*: The lowest temperature during the freezing stage depends on the solidification temperature of the system. The temperature should be at least 2°C lower than the solidification temperature [36]. However, it is common to see from −40 to −50°C as empirical choice for lowest temperature, and while often not necessary also does not normally cause a significant problem. The hold time at the lowest temperature is a function of the fill volume. During development, the product temperature from thermocouple should be monitored as a function of time to determine the time required to reach the lowest desired temperature. In general, 1–2 h hold time is sufficient for fill volumes less than 1 cm and 2–4 h hold time is sufficient for fill volumes more than 1 cm. Fill volumes greater than 2 cm are generally not recommended.
3. *Selection of Annealing Conditions*: Choosing annealing conditions remains somewhat empirical and existing literature provides limited guidance on this aspect. As discussed above, annealing may be carried out with different objectives. If the formulation contains a component that must be crystallized, it has been suggested that annealing should be carried out at a temperature between $T_g'$ and onset of the ice melt endotherm [36]. However, the temperature differential between the two may be quite large. The example shown in Figure 41.2 demonstrates this point where the difference between $T_g'$ and $T_{eu}$ is about 20°C. The exact choice of annealing temperature and time need to be optimized experimentally. Annealing must be carried out at a temperature that (a) is above the $T_g'$ and (b) falls on the crystal growth curve. Therein lies the difficulty as the crystal growth curves are not readily available. For commonly used bulking agents such as mannitol and glycine annealing could be carried out at temperatures between −25 and −20°C for several hours to maximize crystallization, provided the fraction of crystallizing solute is high. If annealing is desired to bring about change in ice morphology and improving batch homogeneity for a totally amorphous system, one needs annealing temperatures relatively close to the onset of melting. It was shown for model amorphous systems such as sucrose and hydroxyethyl starch (HES) that annealing at temperatures between −10 and −2.4°C for 5–10 h was needed for maximum change in primary drying rate and ice morphology [40].
4. *Addressing Scale-Up Issues*: The difference in nucleation temperature between laboratory-scale and production-scale due to change in environmental particulate load could be eliminated if development work were carried out in the same environment. However, this is normally not practical. Therefore, currently, annealing is the only method that has been used to minimize or eliminate supercooling effects in a manufacturing environment. Further development of techniques to control ice nucleation may change this scenario in the future.

## 41.3 DRYING PROCESSES

After freezing, drying is the next step in freeze drying process. Mathematical representation of the drying problem can be described as follows: Once the solution is frozen, the vials are heated by raising the shelf temperature, resulting in sublimation of frozen ice initially and desorption of unfrozen water later. As drying proceeds from top to the bottom of the vial, the dried layers of the cake offer resistance to the water vapor flow due to sublimation of the ice from the layers underneath. The freeze-drying problem is hence a heat transfer (to the vial from shelf and surroundings) and mass transfer (transport of water vapor through porous dried layers and then from the main chamber to the condenser) problem that can be modeled utilizing the fundamentals of heat and mass transfer processes. Further details of the current state of knowledge in modeling this process are described below.

Mathematical modeling of the drying process provides methodology that streamlines experimental screening approaches for developing optimal freeze-drying cycles that produce a quality product in a robust process. A particularly important application of drying process modeling is in the area of freeze-drying process scale-up. A typical scale-up from laboratory-scale to commercial-scale freeze-drying will increase the shelf surface area available for freeze-dryer from 4.5 $ft^2$ to 220 $ft^2$ [52]. Figure 41.4 shows an image of a typical commercial-scale freeze-dryer. Heat transfer may differ, and differences in heterogeneous ice nucleation normally produce significant differences in ice structure and therefore in pore structure of the cake, which impacts mass transfer within the dry layer. Also, differences in dryer design may lead to differences in transport properties between laboratory and commercial dryers. A clear understanding of

**FIGURE 41.4** Image of typical commercial-scale freeze-dryer. This freeze-dryer has a total shelf surface area of 39 $m^2$. It has 24 shelves and 6 trays per shelf. This image is obtained from Pfizer Kalamazoo manufacturing facility.

the dependence of drying kinetics on the heat and mass transfer characteristics of the vial and dried cake, respectively, and the impact of the differences between laboratory scale and commercial scale will facilitate rational scale-up of the freeze-drying process, avoiding expensive failures, and hence will result in efficient development of a robust process, thereby decreasing the cost and time of development [53].

### 41.3.1 Steady-State Heat and Mass Transfer Modeling

Although most reported modeling work uses nonsteady-state modeling techniques, there are some examples describing the use of simple steady-state theory to model the primary drying process. Using the pseudosteady-state approximation, solution of the heat and mass transfer equations has been obtained at several stages during primary drying phase, thus evaluating temperature and pressure profiles as a function of time [33]. Using this simple model, the authors studied the effect of the product temperature on drying time, effects of shelf temperature and chamber pressure were evaluated, and the optimum vial size to minimize primary drying time was identified. This simple model was also utilized to evaluate the effect of process nonuniformities (e.g., variability of vial heat transfer coefficient within the same freeze-drying run, nonuniform shelf temperature, product resistance variation) on the drying times and product temperature during primary drying.

Equations 41.1–41.4 describe a typical freeze-drying process where the solution to be freeze-dried is in a vial, which is placed on top of a temperature-controlled shelf. The steady-state approximation is used, meaning that all of the heat supplied from the shelf is utilized in subliming the ice from the interface [33]. See "Symbols" section for nomenclature details.

$$\frac{dm}{dt} = \frac{A_p \times (P_0 - P_c)}{R_p} \tag{41.1}$$

$$\Delta H_s \times \frac{dm}{dt} = \frac{dQ}{dt} \tag{41.2}$$

$$\frac{dQ}{dt} = A_v \times K_v \times (T_s - T_b) \tag{41.3}$$

$$\Delta H_s \times \frac{P_0 - P_c}{R_p} \times \frac{A_p}{A_v \times K_v} = T_s - T \tag{41.4}$$

**EXAMPLE 41.1**

Sucrose is common excipient used in parenteral formulations. Determine the product temperature during primary drying and length of primary drying time during lyophilizing a sucrose solution at the following given conditions. After building the model, utilize the model to perform an *in silico* robustness test at shelf temperatures that are ±3°C relative to shelf temperature set point and chamber pressure ±50 mTorr relative to the chamber pressure set point.

*Conditions.*

1. Shelf temperature set point ($T_{shelf}$): −25°C
2. Chamber pressure set point ($P_{chamber}$): 100 mTorr
3. Heat of sublimation of ice: 660 cal-$g^{-1}$
4. Average dry layer resistance ($R_p$): 3 $cm^2$-h-Torr-$g^{-1}$
5. Overall heat transfer coefficient between vial and surroundings ($K_v$): 0.00042 cal/(s-$cm^2$-K)
6. Vial dimensions: Inner cross-sectional area = 5.85 $cm^2$; Outer cross-sectional area = 7.08 $cm^2$
7. Formulation details: Solids concentration = 0.05 g solid/g liquid; fill volume = 5 mL

***Solution***

*Part A*. Equation 41.4 can be solved for the unknown interface temperature, $T$, using the given parameters. The solution can be obtained manually or by using the Solver feature in Excel. The interface temperature, $T$, and interface vapor pressure, $P_0$, are related as follows:

$$P_0 = 2.698 \times 10^{10} \times \exp(-6144.96/T)$$

where $T$ is in Kelvin and $P_0$ is the vapor pressure of ice in Torr. Following the above procedure, one finds the average interface temperature is −34.5°C and the primary drying time is 31.5 h. Once $P_0$ is obtained, dm/dt can be calculated using equation 41.1. Total amount of ice to be sublimed ($\Delta m$)

can be calculated from the fill volume and solids concentration. Using these two quantities, time required to sublime all the ice (primary drying time) can be calculated as $\Delta m/(\mathrm{d}m/\mathrm{d}t)$. In a laboratory-scale freeze-drying run (same operating conditions described in this example) with 5 wt% sucrose as the solution (in same vial whose dimensions are described in this example), the product temperature was measured by placing a thermocouple at the bottom of the vial during drying. It was found that the product temperature was −35°C, and the primary drying time was 28 h. The vial was located in the center of the freeze-dryer and the end point of primary drying was considered to be the point when the product temperature reading starts to increase from the steady-state value to reach the shelf temperature set point. One simplification in the above equations is to neglect the difference between the sublimation interface temperature and bottom temperature difference. To obtain more accurate results, this difference can also be accounted for [54].

*Part B*. Now, we have a mathematical model that describes the primary drying process of sucrose. During a manufacturing process operation, set point deviations may occur due to a variety of reasons. The model can be used to predict the effect of set point deviations and thereby test process robustness. Table 41.1 lists the product temperatures and drying times for four extreme deviations from the set points. Also listed in the table are the changes in product temperature and drying time when compared to original set point ($T_{\mathrm{shelf}} = -25°\mathrm{C}$ and $P_{\mathrm{chamber}} = 100\,\mathrm{mTorr}$). As noted above, the model predictions can differ from the experimental values. Therefore, understanding the relative changes in product temperature and drying time as a result of process deviations is one of the useful output from model predictions. Model predictions for the original set point are also listed in Table 41.1. This example demonstrates one of the several ways in which a successful model can be used in lyophilization cycle development to aid in choosing the operating conditions at the laboratory scale and also investigates the robustness of the process.

Recently an interactive modeling tool has been proposed, assuming quasisteady-state heat transfer in frozen layer and in dry product region as well as quasisteady-state mass transfer in the dried layer [55]. This software that is based on a one-dimensional heat and mass transfer model that describes both the primary and the secondary drying stages and also describes the transition region between primary drying and secondary drying. Using this interactive tool, the user can optimize the shelf temperature and/or chamber pressure profile to achieve desired product temperatures.

### 41.3.2 Nonsteady-State Heat and Mass Transfer Modeling

While the simple steady-state models quantitatively describe primary drying, desorption drying (i.e., secondary drying) cannot be accurately described by such models, and several researchers have developed nonsteady-state models of sublimation and desorption. Some advantages of nonsteady-state models include residual moisture prediction as a function of time, and describing the nonsteady-state parts of primary drying (immediately after a change in shelf temperature) [34]. Liapis et al. have presented a sorption–sublimation model to describe the effect of operating conditions on drying times [56, 57]. The initial model, which takes into account heat transfer only from the top surface of the frozen cake [56], has been extended to a more pharmaceutically representative case of heat transfer from both top and bottom surfaces of the frozen cake [57]. One-dimensional energy and material balance equations for frozen and dried layers were solved. Utilizing this mathematical model, the authors could calculate the sorbed water concentration profiles at the end of primary drying at different positions in the cake as a function of different operating conditions. A further comparison of the performance of different mathematical models for predicting sorbed water concentrations as a function of time was also provided [58]. The authors utilize the one-dimensional mathematical model to predict optimal operating conditions in a freeze-drying cycle. This mathematical model of sublimation and desorption drying was further extended to model the primary and secondary drying stages in vial lyophilization, which is a more realistic

**TABLE 41.1 Evaluation of Effect of Change in Shelf Temperature and Chamber Pressure Changes on Product Temperature During Primary Drying and Primary Drying Time**

| $T_{\mathrm{shelf}}$ (°C) | $P_{\mathrm{chamber}}$ (mTorr) | Product Temperature (°C) | $\Delta T$ (Product Temperature at New Condition - Product Temperature at Original Conditions) (°C) | Drying Time (h) | Δtime (Drying Time at New Condition - Drying Time at Original Conditions) (h) |
|---|---|---|---|---|---|
| −25 | 100 | −34.5 | 0 | 31.5 | 0 |
| −22 | 50 | −35.5 | −1 | 22 | −9.5 |
| −22 | 150 | −32 | 2.5 | 30 | −1.5 |
| −28 | 50 | −37.5 | −3 | 31.5 | 0 |
| −28 | 150 | −33.5 | 1 | 53 | 21.5 |

representation of a typical pharmaceutical freeze-drying process [59, 60]. A further application of modeling was in understanding the mechanism of bound water removal utilizing one-dimensional nonsteady-state modeling of both primary and secondary drying stages [61]. Using the mathematical model coupled with experimental confirmation, they conclude that the removal of bound water during primary drying portion of freeze-drying is negligible.

A further improvement of the one-dimensional model was made by extending it to a two-dimensional system [62]. A finite element method was used to solve two-dimensional heat and mass transfer equations for the frozen and dried layers. Accounting for the removal of ice and sorbed water, this model predicts the position and geometric shape of the moving interface, thus modeling the entire primary and secondary drying stages. A physical rationale for the choice of boundary conditions used is provided elsewhere [34]. The authors further evaluate the model predictions using experimental results suggesting the usefulness of the utilizing mathematical modeling in freeze-drying process development [34]. An example for nonsteady-state model equations is shown below. Equations 41.5–41.11 are intended to give the reader a sense for the nonsteady-state formulation of the freeze-drying problem. Equation 41.5 describes the water vapor flow in the dry layer. This equation can be summarized as the sum of change in water concentration in the gas phase and the change in water concentration in the solid phase equals the flux of water out of the system. Equations 41.6 and 41.7 describe the change in water content of the solid phase and molar water flux in the dried region. Equation 41.6 assumes that the rate of change in water content of the solid phase is proportional to the difference between the water content and the equilibrium water content at the surrounding water activity, $a_w$, at temperature $T$, denoted $C^*(a_w,T)$ where $k_g$ is a "rate constant" assumed to exhibit Arrhenius temperature dependence. The terms on the right-hand side of equation 41.7 represent the contributions of both diffusion and bulk fluid flow to the water flux. Bulk fluid flow is mostly Knudsen flow in usual pharmaceutical freeze-drying applications. Further simplification of equation 41.7 is possible by considering the fact that vapor composition in the cake and in the drying chamber during practical primary drying situation is nearly 100% water vapor, we can ignore diffusion in the dry layer during primary drying leaving only bulk flow or Knudsen flow as primary contributor to water vapor flux. These simplifications are described in Ref. 34.

Equations 41.9–41.11 describe the heat transfer in dried layer and frozen layer. Equation 41.9 describes the heat transfer in dry layer, which is conservation of energy in dry layer. Energy conservation for frozen layer leads to equation 41.10. Equation 41.11 is the conservation of energy at the sublimation interface, where rates of heat flow into the interface from dry and frozen layers is compensated by the rates of heat removed by gas flow and sublimation. As mentioned above, complete details and further simplifications of these equations can be found in Ref. 34.

#### *41.3.2.1 Nonsteady-State Model Equations Representing Freeze-Drying (see "Symbols" Section)*

$$\varepsilon \frac{\partial C_{w,g}}{\partial t} + \rho_I \frac{\partial C_{w,s}}{\partial t} = -\nabla \cdot N_w \tag{41.5}$$

$$\frac{\partial C_{w,s}}{\partial t} = -k_g\left(C_{w,s} - C^*(a_w, T)\right) \tag{41.6}$$

$$N_w = -k_1 \nabla C_{w,g} - k_2 C_{w,g} \nabla P \tag{41.7}$$

$$N_w = -\frac{M_w}{RT} \cdot K_w \left(1 + \frac{C_{01} P_w}{K_w \mu_{mx}}\right) \nabla P_w \approx -\frac{M_w}{RT} \cdot K_w \nabla P_w \tag{41.8}$$

$$\rho_I C_{pI} \frac{\partial T}{\partial t} = k_I \nabla^2 T + \rho_I \Delta H_v \frac{\partial C_{w,s}}{\partial T} - C_{p,g} \nabla (N_t T) \tag{41.9}$$

$$\rho_{II} C_{PII} \frac{\partial T}{\partial t} = k_{II} \nabla^2 T \tag{41.10}$$

$$-k_I \left(\frac{\partial T}{\partial n}\right)_I + k_{II} \left(\frac{\partial T}{\partial n}\right)_{II} = -N_{t_n} C_{p,g} T - N_{w_n} \Delta H_s \tag{41.11}$$

Utilization of mathematical modeling techniques described above will result in greater understanding of the effect of process variables on the quality of the product. These modeling tools provide an excellent opportunity to apply the quality by design principles to ensure that quality of the freeze-dried product is built into the process. One such practical industrial application of mathematical modeling of freeze-drying is demonstrated in freeze-drying of Azithromycin solution [63]. The authors have confirmed the model predictions of the PASSAGE software [34, 62][2] and further utilized the mathematical model to predict the operating conditions at pilot scale to achieve a product temperature profile that is equivalent to the profile achieved for an optimized laboratory-scale lyophilization cycle. This work demonstrated the utility of the numerical models in the area of scale-up and optimization of lyophilization cycles at commercial scale [63].

Several other modeling approaches and applications have been reported in the literature that describe the freeze-drying process utilizing fundamental heat and mass transfer models [64–70]. These reports demonstrate that the fundamental understanding of the drying stage has evolved extensively

[2] PASSAGE is commercially available freeze-drying software capable to solving unsteady state mass and heat transfer equations. This is commercially available from Technalysis, Inc.

and scientists can utilize these techniques to rapidly develop optimized lyophilization cycles.

### 41.3.3 Determination of Modeling Parameters: Dry Layer Resistance and Heat Transfer Coefficient

The importance of heat transfer coefficient and mass transfer resistance during drying, especially for modeling purposes should now be evident to the reader. The manometric temperature measurement (MTM) procedure is one of the techniques that is useful in estimation of the mass transfer resistance offered by the dried layer and stopper.

In the MTM method, the flow of water vapor from the product chamber to condenser is momentarily interrupted during primary drying by quickly closing the valve separating the chamber and condenser, resulting in an increase in chamber pressure due to sublimation [71]. This transient increase in chamber pressure is modeled by considering the several factors contributing to the pressure rise. A curvilinear regression estimates the vapor pressure of ice and resistance offered by dried layer. The capabilities of this modeling technique have been further examined in estimation of product temperature [54], measurement of dry layer resistance [72], and heat and mass transfer measurements, including the vial heat transfer coefficient [73].

An "expert system" (SMART) that will allow development of an optimized freeze-drying process during laboratory-scale development in one experiment is another application of the MTM technique [74]. SMART is an excellent example of the utilization of heat and mass transfer theory and modeling to facilitate the development of freeze-drying cycle conditions. Measurement of product resistance and vapor pressure of ice by MTM allows calculation of the sublimation rate [71], which is then used to optimize the shelf temperature settings. Figure 41.5 summarizes the SMART concept. The expert systems algorithms control the different parts of the freeze-drying. Freezing conditions are chosen based on the input parameters regarding formulation details. Primary drying conditions are chosen based on the MTM feedback. Also, the algorithm chooses conditions for secondary drying based on input parameters. A detailed description can found in Ref. 74. A variation of the original MTM approach, denoted "pressure rise analysis (PRA)," was proposed as an improvement to the original MTM algorithm [75]. Using this PRA model, the authors estimate the same parameters as obtained by MTM, sublimation front temperature, resistance offered by dry layer, and the overall vial heat transfer coefficient. Utility of SMART and MTM during the lyophilization cycle development has been demonstrated in measuring product resistance, predicting product temperature and primary drying time [76].

Another method, based on an analysis of the normal product temperature history during primary drying, has been suggested as a method to obtain product resistance data without doing special experiments, such as the MTM experiment [77]. This technique once again utilizes the understanding of heat and mass transfer mechanisms to determine desired parameters (mass transfer resistance) of the formulation during freeze-drying. Other techniques utilize similar applications of heat and mass transfer fundamentals to estimate mass transfer resistances during freeze-drying [78–80]. Recently, another variation of the original MTM approach was suggested as a more rigorous model for describing the pressure rise during the valve closing procedure [81]. The stated final goal of using this advanced approach is to develop an online tool for controlling the heating strategy during freeze-drying, and the same group recently reported an online monitoring system (and hence control) for primary drying phase of lyophilization as a further application of the mathematical modeling [82]. This system provides in-line control signals (adjusting shelf heating fluid temperature throughout primary drying),

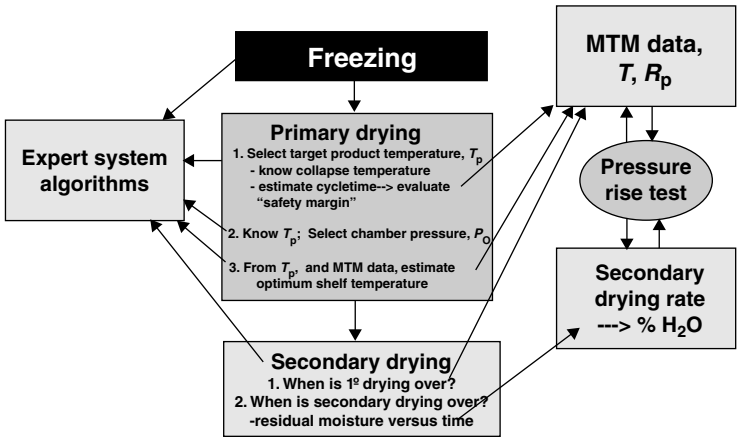


**FIGURE 41.5** Summary of the "SMART" Freeze-Dryer concept. Reproduced from Ref. 74 with permission from Springer.

utilizing simple heat and mass transfer algorithm in conjunction with measurements made during the freeze-drying process to achieve desired product and process performance. While this general procedure is identical to that employed by the MTM procedure within the SMART Freeze-Dryer technology, the details of the heat and mass transfer analysis do differ. Further details can be found in Ref. 82.

Another important input parameter for models is the heat transfer coefficient of the vial. This parameter can be determined both by performing simple water sublimation experiments in the laboratory as a function of chamber pressure [83] and by MTM measurements (or variations on the MTM technique) as noted above.

Successful model development for the drying process depends on the accuracy of the modeling parameters. Dry layer resistance and heat transfer coefficient are two critical parameters. While one might estimate these quantities from an existing database, ideally these parameters should be measured for the application of interest, particularly with the dry layer resistance that varies considerably between products and is relatively difficult to quantitatively predict.

### 41.3.4 Issues in Scale-Up of Freeze-Drying Process

The heat transfer coefficient of a given vial depends not only on the bottom contour of the vial but also on the location of the vial within the vial array in a given freeze-dryer. Heat is transferred between shelf and vial due to three mechanisms: heat transfer from the contact area between the vial and the shelf, conduction of gas molecules between vial bottom and shelf surface, and due to radiation. While the first two modes of heat transfer can be considered independent of the location of the vial, the radiative heat transfer depends on the location of the vial. Edge vials have a greater area of exposure to radiation heat transfer (i.e., part of the side as well as top and bottom) and often the chamber surfaces that are responsible for side radiation are hotter than the shelf surface. These effects result in differences in heat transfer coefficients between center and edge vials [84, 85]. Understanding the impact of such heat transfer coefficient variation on the drying performance will help the scientist design the process so as to achieve optimal product irrespective of its location in the freeze-dryer. A multidimensional unsteady-state modeling was utilized to determine the effect of location of the vials in freeze-dryer on the overall drying time temperature distribution [86]. This study shows the importance of wall temperature in influencing the drying characteristics in vials located at different positions in a freeze-dryer.

Another important challenge in the freeze-drying process is the scale-up of lyophilization cycles from laboratory to pilot to commercial-scale dryers. The edge vial effect can be scale dependent. The heat and mass transfer issues during freeze-drying process development have been summarized in an excellent review, Ref. 87. In addition to providing a review of heat and mass transfer mechanisms to be considered during freeze-drying cycle development the authors also discuss the related scale-up issues. As mentioned above, radiative heat transfer varies dues to the location of the vial in the freeze-dryer. This radiation effect is also different from a laboratory dryer to pilot or a commercial-scale dryer. Differences in percentage of edge vials and differences in wall temperatures and differences in emissivities between laboratory scale and manufacturing scale introduce scale-up differences that can be significant. For example, a front vial in a laboratory freeze-dryer can receive $\approx$1.8 times greater heat transfer than a corresponding vial in a manufacturing freeze-dryer [29]. This additional heat input will directly affect the product temperature and drying time. Hence, understanding these differences between freeze-dryers is essential to proper scale-up. Another important scale based difference is the temperature distribution across the freeze-dryer shelf. Differences between the shelf temperature set point and measured shelf surface temperature as a function of the sublimation rate are reported [29]. These differences can be dryer specific in that dryer design and heat transfer characteristics of the fluid can cause shelf surface temperature differences between different freeze-dryers even at identical thermal loads. A properly designed shelf mapping study can determine the magnitude of the expected effects [87]. These differences between laboratory-scale and production-scale dryers have been highlighted and a step-by-step systematic approach to correlate dryers at two scales leading toward a successful scale-up are discussed in Ref. 52.

It should be obvious that the application of engineering principles of heat and mass transfer modeling and scale-up adjustments are essential to the successful design of a freeze-drying process for manufacturing. Utilizing these engineering principles will facilitate a rationale lyophilization cycle development and scale-up effort. The "general rules" for successful process design and scale-up can be summarized as follows:

1. Select the optimal freezing conditions that results in an ice morphology that is uniform within a given vial, uniform between vials in the same batch, uniform between batches, and uniform from laboratory to manufacturing. In addition, a structure composed of larger ice crystals is advantageous in that such a structure produces lower product resistance and faster primary drying.
2. Utilize the understanding of the heat and mass transfer mechanisms during drying to select the primary and secondary conditions to achieve maximal drying rate (minimal drying time) while maintaining the product temperature below the critical product temperature.
   (a) Utilize the techniques described in literature to measure heat transfer coefficient of the vial of interest.

(b) Determine the resistance offered by dry layer during the drying stage.

(c) Utilizing mathematical models obtain initial estimates for the first laboratory cycle and then optimize the cycle conditions using the SMART Freeze-Dryer methodology (or equivalent) and/or a few experiments to confirm results.

3. Understand the freeze-dryer differences with respect to the heat and mass transfer mechanisms during scale-up and utilize mathematical models to estimate the cycle conditions at larger scale.

Some examples of application of these concepts for rationale scale-up have been reported in literature [63, 88, 89]. Heat and mass transfer models in conjunction with limited lyophilization runs were utilized to successfully determine heat transfer coefficients and to evaluate the robustness of the lyophilization cycle at different operating conditions [88]. A systematic approach by utilizing laboratory-scale experiments to determine heat and mass transfer coefficients and mathematical modeling to predict operating conditions at pilot scale thus minimizing the number of pilot scale runs has also been reported [63]. Hopefully, increased use of theoretical modeling will be a norm in the future as increased emphasis is placed on "quality by design."

### 41.3.5 Mass Flow from Chamber to Condenser

Many advancements in modeling the sublimation and desorption of water vapor within the vial have been made as discussed in the Sections 41.3.1–41.3.4. The literature on modeling the flow of water vapor once it leaves the vial, that is, from chamber to condenser is, however, sparse. The lyophilization process can be limited by mass transfer within the freeze-dryer at high sublimation load [90]. In addition, freeze-dryer design differences at different scales may lead to different product temperature profiles that may not be captured in vial modeling. Therefore, it is important that these factors be captured in the models for freeze-drying. Some recent publications have described the use of various tools to model vapor flow in the freeze-dryer. Most of the work cited has used computational fluid dynamics (CFD) for this purpose. The effect of some geometrical parameters of the drying chamber such as clearances between the shelves and the position of the duct between the chamber and the condenser on the global fluid dynamics of the sublimated vapor in both small-scale and industrial-scale drying chambers were investigated as a function of the sublimation rate [91]. It was concluded that local pressure differentials existed in the freeze-dryer and contributed to heterogeneity in sublimation rate in addition to the commonly known effects such as radiation effects. These effects were more pronounced in larger scale freeze-dryers. However, the mag-

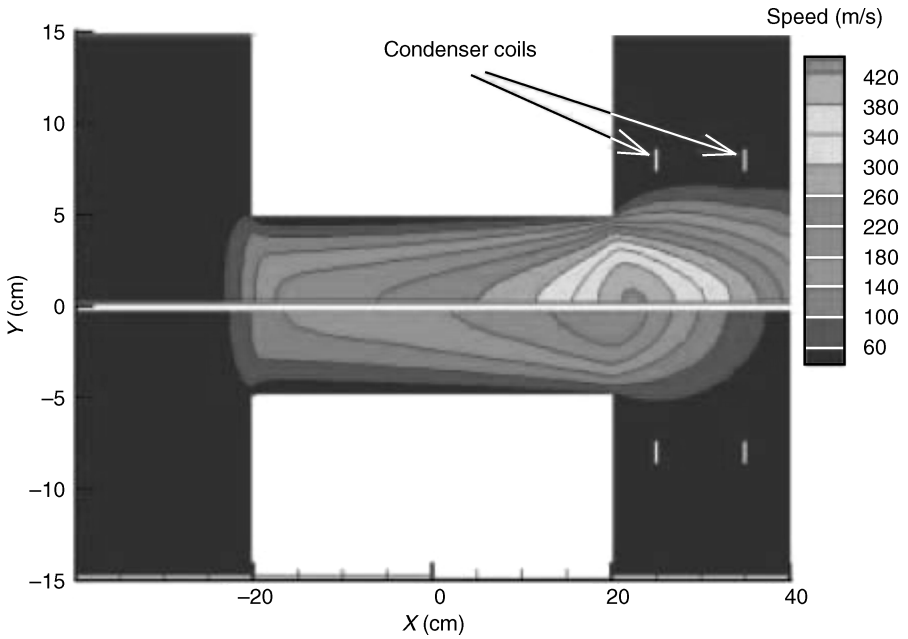


**FIGURE 41.6** Velocity profile of water vapor in laboratory-scale freeze-dryer. The top half shows the results for 50 mTorr chamber pressure and choked flow conditions at the condenser entrance are apparent. The lower half shows simulation for 30 mTorr. The vapor velocity in this case remains below the Mach I limit. The data show potential choked flow conditions for some operating parameters. Reprinted from Ref. 91 with permission of Wiley-Liss, Inc., a subsidiary of John Wiley & Sons, Inc.

nitude of these effects was not explicitly discussed. It has been documented that the duct between the drying chamber and the condenser may be a bottleneck at high sublimation rates [90]. This effect has been called choked flow, and CFD has been employed to identify critical variables impacting choked flow [92]. It was determined that ratio of chamber to condenser pressure determined the onset of choked flow. Recently, a more comprehensive model that includes the drying chamber, duct, and condenser using CFD has been published [93]. The Knudsen number (*Kn*), a dimensionless parameter, has been used to define the flow regime and various equations that are valid in different flow regimes have been described. *Kn* is the ratio of the molecular mean free path (λ) and characteristic length scale of flow (*L*). For example, Navier–Stokes equation has been used where *Kn* is below 0.01 and continuum hypothesis is valid, that is, one is dealing with fluid flow or "viscous flow." The Boltzmann equation has been used in rarefied or "free molecular flow" regime ($Kn > 0.1$). A new approach to solving the Boltzmann equation using a statistical direct simulation Monte Carlo (DSMC) method has been described. Differences between a laboratory-scale and industrial-scale freeze- dryer, especially the impact of CIP/SIP (clean in place/steam in place) line in industrial freeze-dryer, on the fluid flow were presented. Simulation of water vapor flow in the freeze-dryer also showed choked flow conditions may exist at the point of maximum flow velocity, which is along the axis of the duct at the entrance to the condenser. Figure 41.6 shows the simulation for two different chamber pressures. The top half shows the results for 50 mTorr chamber pressure and choked flow conditions at the condenser entrance are apparent. The lower half shows simulation for 30 mTorr. The vapor velocity in this case remains below the Mach I limit. It has therefore been argued that computational fluid flow studies may also be useful in the design of freeze-dryers.

Following the guidelines presented in this chapter and the references cited herein, it should result in systematic approach to freeze-drying process development and scale-up. Increased use of modeling wherever applicable will be consistent with the "quality by design" philosophy.

## SYMBOLS

### Steady-State Model Equations

| | |
|---|---|
| $dm/dt$ | sublimation rate |
| $A_p$ | inner cross-sectional area of the vial |
| $P_0$ | vapor pressure of ice at interface temperature |
| $P_c$ | chamber pressure |
| $R_P$ | dry layer resistance |
| $dQ/dt$ | rate of heat transfer |
| $A_v$ | outer cross-sectional area of the vial |
| $K_v$ | heat transfer coefficient between the vial and the surroundings (includes heat transfer form shelf contact and also radiation) |
| $T_s$ | shelf temperature |
| $T_b$ | product temperature at the bottom of the vial |
| T | product temperature at the sublimation interface |
| $\Delta H_s$ | heat of sublimation of ice |

### Nonsteady-State Model Equations

| | |
|---|---|
| $\varepsilon$ | void fraction in the dried region |
| $\rho_I$ | density of dry region |
| $C_{w,s}$ | concentration of sorbed water |
| $N_w$ | molar flux of water |
| $k_g$ | mass transfer coefficient for desorption |
| $C^*$ | equilibrium concentration of sorbed water |
| $a_w$ | water activity |
| $T$ | temperature |
| $k_1$ | bulk diffusivity constant |
| $k_2$ | self diffusivity constant |
| $P$ | total pressure |
| $C_{pI}$ | heat capacity of dry layer |
| $k_I$ | thermal conductivity of dry layer |
| $\Delta H_v$ | heat of vaporization of sorbed water |
| $\rho_{II}$ | density of the frozen region |
| $C_{PII}$ | heat capacity of frozen region |
| $k_{II}$ | thermal conductivity of frozen layer |
| $N_{w_n}$ | molar flux of water, normal component |
| $\Delta H_s$ | heat of sublimation of ice |

## REFERENCES


1. Brange J. *Galenics of Insulin*, 1st edition, Springer, 1987.
2. Pikal MJ, Lukes AL, Lang JE. Thermal decomposition of amorphous β-lactam antibacterials. *J. Pharm. Sci.* 1977;66(9):1312–1316.
3. Pikal MJ, Lukes AL, Lang JE, Gaines K. Quantitative crystallinity determinations for β-lactam antibiotics by solution calorimetry: correlations with stability. *J. Pharm. Sci.* 1978;67(6):767–773.
4. Pikal MJ, Dellerman KM. Stability testing of pharmaceuticals by high-sensitivity isothermal calorimetry at 25°C: cephalosporins in the solid and aqueous solution states. *Int. J. Pharm.* 1989;50(3):233–252.
5. Pikal MJ, Rigsbee DR. The stability of insulin in crystalline and amorphous solids: observation of greater stability for the amorphous form. *Pharm. Res.* 1997;14(10):1379–1387.
6. Pikal MJ. Freeze-drying of proteins. Part II. Formulation selection. *BioPharm* 1990;3(9):26–30.
7. Pikal MJ. Freeze-drying of proteins. Part I. Process design. *BioPharm* 1990;3(8):18–20, 22–24, 26–28.
8. Pikal MJ. Freeze-drying of proteins: process, formulation, and stability. *ACS Symp. Ser.* 1994;567:120–133.

9. MacKenzie AP. Factors affecting the transformation of ice into water vapor in the freeze-drying process. *Ann. N.Y. Acad. Sci.* 1965;125:522–547.
10. Broadhead J, Rouan SKE, Rhodes CT. The spray drying of pharmaceuticals. *Drug Dev. Ind. Pharm.* 1992;18(11–12): 1169–1206.
11. Mumenthaler M, Hsu CC, Pearlman R. Feasibility study on spray-drying protein pharmaceuticals: recombinant human growth hormone and tissue-type plasminogen activator. *Pharm. Res.* 1994;11(1):12–20.
12. Masters K. Applications of spray-drying in the food industry, in the pharmaceutical-biochemical industry. In: *Spray-Drying Handbook*, Longman Scientific and Technical, Essex, UK, 1991, pp. 491–676.
13. Franks F. Solid aqueous solutions. *Pure Appl. Chem.* 1993; 65(12):2527–2537.
14. Roser B. Trehalose drying: a novel replacement for freeze-drying. *BioPharm* 1991;4(8):47–53.
15. Abdul-Fattah AM, Kalonia DS, Pikal MJ. The challenge of drying method selection for protein pharmaceuticals: product quality implications. *J. Pharm. Sci.* 2007;96(8): 1886–1916.
16. Levine H, Slade L. Another view of trehalose for drying and stabilizing biological materials. *BioPharm* 1992;5(4):36–40.
17. Pregnolato FC. *Proceedings of the International Congress, Advanced Technologies for Manufacturing of Asceptic and Terminally Sterilized Pharmaceuticals and Biopharmaceuticals*, Basel, Switzerland, 1992, pp 4–30.
18. Carpenter JF, Crowe JH, Arakawa T. Comparison of solute-induced protein stabilization in aqueous solution and in the frozen and dried states. *J. Dairy Sci.* 1990; 73(12):3627–3636.
19. Tanaka K, Takeda T, Miyajima K. Cryoprotective effect of saccharides on denaturation of catalase by freeze-drying. *Chem. Pharm. Bull.* 1991;39(5):1091–1094.
20. Hellman K, Miller DS, Cammack KA. The effect of freeze-drying on the quaternary structure of L-asparaginase from *Erwinia carotovora*. *Biochim. Biophys. Acta, Protein Struct. Mol. Enzymol.* 1983;749(2):133–142.
21. Ressing ME, Jiskoot W, Talsma H, Van Ingen CW, Beuvery EC, Crommelin DJA. The influence of sucrose, dextran, and hydroxypropyl β-cyclodextrin as lyoprotectants for a freeze-dried mouse IgG2a monoclonal antibody (MN12). *Pharm. Res.* 1992;9(2):266–270.
22. Izutsu K-I, Yoshioka S. Stabilization of protein pharmaceuticals in freeze-dried formulations. *Drug Stab*. 1995;1 (1):11–21.
23. Bell LN, Hageman MJ. Differentiating between the effects of water activity and glass transition dependent mobility on a solid state chemical reaction: aspartame degradation. *J. Agric. Food Chem.* 1994;42(11):2398–2401.
24. Pikal MJ, Dellerman KM, Roy MI, Riggin RM. The effects of formulation variables on the stability of freeze-dried human growth hormone. *Pharm. Res.* 1991;8(4):427–436.
25. Pikal MJ, Dellerman K, Roy ML. Formulation and stability of freeze-dried proteins: effects of moisture and oxygen on the stability of freeze-dried formulations of human growth hormone. *Dev. Biol. Stand.* 1992;74:21–38.
26. Townsend MW, DeLuca P.P. Use of lyoprotectants in the freeze-drying of a model protein, ribonuclease A. *J. Parenter. Sci. Technol.* 1988;42(6):190–199.
27. Prestrelski SJ, Pikal KA, Arakawa T. Optimization of lyophilization conditions for recombinant human interleukin-2 by dried-state conformational analysis using Fourier-transform infrared spectroscopy. *Pharm. Res.* 1995;12(9): 1250–1259.
28. Roy ML, Pikal MJ, Rickard EC, Maloney AM. The effects of formulation and moisture on the stability of a freeze-dried monoclonal antibody-vinca conjugate: a test of the WLF glass transition theory. *Dev. Biol. Stand.* 1992;74:323–340.
29. Rambhatla S, Tchessalov S, Pikal Michael J. Heat and mass transfer scale-up issues during freeze-drying. III. Control and characterization of dryer differences via operational qualification tests. *AAPS PharmSciTech* 2006;7(2):E39.
30. Roy ML, Pikal MJ. Process control in freeze drying: determination of the end point of sublimation drying by an electronic moisture sensor. *J Parenter Sci Technol* 1989, 43, (2):60–6.
31. Searles, JA, Carpenter, JF, Randolph, TW. The ice nucleation temperature determines the primary drying rate of lyophilization for samples frozen on a temperature-controlled shelf, *J. Pharm. Sci.* 2001; 90(7):860–871.
32. Rambhatla S, Ramot R, Bhugra C, Pikal Michael J. Heat and mass transfer scale-up issues during freeze drying. II. Control and characterization of the degree of supercooling. *AAPS PharmSciTech* 2004;5(4):e58.
33. Pikal MJ. Use of laboratory data in freeze drying process design: heat and mass transfer coefficients and the computer simulation of freeze drying. *J. Parenter. Sci. Technol.* 1985; 39(3):115–139.
34. Pikal MJ, Cardon S, Bhugra C, Jameel F, Rambhatla S, Mascarenhas WJ, Akay HU. The nonsteady state modeling of freeze drying: in-process product temperature and moisture content mapping and pharmaceutical product quality applications. *Pharm. Dev. Technol.* 2005;10(1); 17–32.
35. Gilra NK. Homogeneous nucleation temperature of supercooled water. *Phys. Lett. A* 1968;28(1):51–52.
36. Tang X, Pikal MJ. Design of freeze-drying processes for pharmaceuticals: practical advice. *Pharm. Res.* 2004; 21(2):191–200.
37. Pikal MJ, Shah S. The collapse temperature in freeze drying: dependence on measurement methodology and rate of water removal from the glassy phase. *Int. J. Pharm.* 1990; 62(2–3):165–186.
38. Chatterjee K, Shalaev EY, Suryanarayanan R. Partially crystalline systems in lyophilization. II. Withstanding collapse at high primary drying temperatures and impact on protein activity recovery. *J. Pharm. Sci.* 2005;94(4); 809–820.
39. Milton N, Nail SL. The physical state of nafcillin sodium in frozen aqueous solutions and freeze-dried powders. *Pharm. Dev. Technol.* 1996;1(3):269–277.
40. Searles JA, Carpenter JF, Randolph TW. Annealing to optimize the primary drying rate, reduce freezing-induced drying rate

heterogeneity, and determine $T_g'$ in pharmaceutical lyophilization. *J. Pharm. Sci.* 2001;90(7):872–887.

41. Chouvenc P, Vessot S, Andrieu J. Experimental study of the impact of annealing on ice structure and mass transfer parameters during freeze-drying of a pharmaceutical formulation. *PDA J. Pharm. Sci. Technol.* 2006;60(2):95–103.
42. Lu X, Pikal Michael J. Freeze-drying of mannitol-trehalose-sodium chloride-based formulations: the impact of annealing on dry layer resistance to mass transfer and cake structure. *Pharm. Dev. Technol.* 2004;9(1):85–95.
43. Pikal MJ, Shah S, Roy ML, Putman R. The secondary drying stage of freeze drying: drying kinetics as a function of temperature and chamber pressure. *Int. J. Pharm.* 1990; 60(3):203–217.
44. Heller MC, Carpenter JF, Randolph TW. Manipulation of lyophilization-induced phase separation: implications for pharmaceutical proteins. *Biotechnol. Prog.* 1997;13(5):590–596.
45. Rowe TD. *A technique for nucleation of ice.* International Symposium on Biological Product Freeze-Drying and Formulation, Geneva, Switzerland, 1990.
46. Nakagawa K, Hottot A, Vessot S, Andrieu J. Influence of controlled nucleation by ultrasounds on ice morphology of frozen formulations for pharmaceutical proteins freeze-drying. *Chem. Eng. Process* 2006;45(9):783–791.
47. Petersen A, Rau G, Glasmacher B. Reduction of primary freeze-drying time by electric field induced ice nucleus formation. *Heat Mass Transf.* 2006;42(10):929–938.
48. Petersen A, Schneider H, Rau G, Glasmacher B. A new approach for freezing of aqueous solutions under active control of the nucleation temperature. *Cryobiology* 2006;53 (2):248–257.
49. Liu J, Viverette T, Virgin M, Anderson M, Dalal P. A study of the impact of freezing on the lyophilization of a concentrated formulation with a high fill depth. *Pharm. Dev. Technol.* 2005;10(2):261–272.
50. Kramer M, Sennhenn B, Lee G. Freeze-drying using vacuum-induced surface freezing. *J. Pharm. Sci.* 2002;91(2):433–443.
51. Nakagawa K, Hottot A, Vessot S, Andrieu J. Modeling of freezing step during freeze-drying of drugs in vials. *AIChE J.* 2007;53(5):1362–1372.
52. Kuu WY, Hardwick LM, Akers MJ. Correlation of laboratory and production freeze drying cycles. *Int. J. Pharm.* 2005; 302(1–2):56–67.
53. Sadikoglu H, Ozdemir M, Seker M. Freeze-drying of pharmaceutical products: research and development needs. *Drying Technol.* 2006;24(7):849–861.
54. Tang X, Nail Steven L, Pikal Michael J. Evaluation of manometric temperature measurement, a process analytical technology tool for freeze-drying. Part I. Product temperature measurement. *AAPS PharmSciTech* 2006;7(1):E14.
55. Trelea IC, Passot S, Fonseca F, Marin M. An interactive tool for the optimization of freeze-drying cycles based on quality criteria. *Drying Technol.* 2007;25(5):741–751.
56. Litchfield RJ, Liapis AI. An adsorption–sublimation model for a freeze dryer. *Chem. Eng. Sci.* 1979;34(9):1085–1090.
57. Millman MJ, Liapis AI, Marchello JM. An analysis of the lyophilization process using a sorption–sublimation model and various operational policies. *AIChE J.* 1985; 31(10):1594–604.
58. Liapis AI, Marchello JM. Advances in the modeling and control of freeze-drying. *Adv. Drying* 1984;3:217–244.
59. Liapis AI, Bruttini R. Freeze-drying of pharmaceutical crystalline and amorphous solutes in vials: dynamic multi-dimensional models of the primary and secondary drying stages and qualitative features of the moving interface. *Drying Technol.* 1995;13(1):43–72.
60. Sheehan P, Liapis AI. Modeling of the primary and secondary drying stages of the freeze drying of pharmaceutical products in vials: numerical results obtained from the solution of a dynamic and spatially multi-dimensional lyophilization model for different operational policies. *Biotechnol. Bioeng.* 1998; 60(6):712–728.
61. Sadikoglu H, Liapis AI. Mathematical modeling of the primary and secondary drying stages of bulk solution freeze-drying in trays: parameter estimation and model discrimination by comparison of theoretical results with experimental data. *Drying Technol.* 1997;15(3–4):791–810.
62. Mascarenhas WJ, Akay HU, Pikal MJ. A computational model for finite element analysis of the freeze-drying process. *Comput. Mehtods Appl. Mecha. Eng.* 1997;148:105–124.
63. Kramer T, Kremer DM, Pikal MJ, Petre WJ, Shalaev EY, Gatlin LA. A procedure to optimize scale-up for the primary drying phase of lyophilization. *J. Pharm. Sci.* 2009;98(1):307–318.
64. Nastaj J, Witkiewicz K. Numerical model of freeze drying of random solids at two-region conductive–radiative heating. *Inz. Chem. Procesowa* 2004;25(1):109–121.
65. Boss EA, Maciel Filho R, II, Vasco de Toledo EC, III. Freeze drying process: real time model. *Tech. Pap. ISA* 2002l;426:59–70.
66. Tu W, Chen M, Yang Z, Chen H. A mathematical model for freeze-drying. *Chin. J. Chem. Eng.* 2000;8(2):118–122.
67. Kisakurek B, Celiker H. A modified moving boundary model for freeze-dryers. *Proc. Int. Drying Symp.* 1984;2:420–424.
68. Hottot Al, Peczalski R, Vessot S, Andrieu J. Freeze-drying of pharmaceutical proteins in vials: modeling of freezing and sublimation steps. *Drying Technol.* 2006;24(5):561–570.
69. Boss EA, Filho RM, de Toledo ECV. Freeze drying process: real time model and optimization. *Chem. Eng. Process.* 2004; 43(12):1475–1485.
70. Velardi SA, Barresi AA. Development of simplified models for the freeze-drying process and investigation of the optimal operating conditions. *Chem. Eng. Res. Des.* 2008;86(1):9–22.
71. Milton N, Pikal MJ, Roy ML, Nail SL. Evaluation of manometric temperature measurement as a method of monitoring product temperature during lyophilization. *PDA J. Pharm. Sci. Technol.* 1997;51(1):7–16.
72. Tang Xiaolin C, Nail Steven L, Pikal Michael J. Evaluation of manometric temperature measurement, a process analytical technology tool for freeze-drying. Part II. Measurement of dry-layer resistance. *AAPS PharmSciTech* 2006;7(4):93.

73. Tang Xiaolin C, Nail Steven L, Pikal Michael J. Evaluation of manometric temperature measurement (MTM), a process analytical technology tool in freeze drying. Part III. Heat and mass transfer measurement. *AAPS PharmSciTech* 2006;7(4):97.
74. Tang X, Nail SL, Pikal MJ. Freeze-drying process design by manometric temperature measurement: design of a SMART Freeze-Dryer. *Pharm. Res.* 2005;22(4):685–700.
75. Chouvenc P, Vessot S, Andrieu J, Vacus P. Optimization of the freeze-drying cycle: a new model for pressure rise analysis. *Drying Technol.* 2004;22(7):1577–1601.
76. Gieseler H, Kramer T, Pikal MJ. Use of manometric temperature measurement (MTM) and SMART Freeze-Dryer technology for development of an optimized freeze-drying cycle. *J. Pharm. Sci.* 2007;96(12):3402–3418.
77. Kuu WY, Hardwick LM, Akers MJ. Rapid determination of dry layer mass transfer resistance for various pharmaceutical formulations during primary drying using product temperature profiles. *Int. J. Pharm.* 2006;313(1–2); 99–113.
78. Pikal MJ, Shah S, Senior D, Lang JE. Physical chemistry of freeze-drying: measurement of sublimation rates for frozen aqueous solutions by a microbalance technique. *J. Pharm. Sci.* 1983;72(6):635–650.
79. Kuu W-Y, McShane J, Wong J. Determination of mass transfer coefficients during freeze drying using modeling and parameter estimation techniques. *Int. J. Pharm.* 1995;124(2):241–252.
80. Zhai S, Su H, Taylor R, Slater NKH. Pure ice sublimation within vials in a laboratory lyophiliser; comparison of theory with experiment. *Chem. Eng. Sci.* 2005;60(4):1167–1176.
81. Velardi SA, Rasetto V, Barresi AA. Dynamic parameters estimation method: advanced manometric temperature measurement approach for freeze-drying monitoring of pharmaceutical solutions. *Ind. Eng. Chem. Res.* 2008;47(21):8445–8457.
82. Barresi AA, Pisano R, Fissore D, Rasetto V, Velardi SA, Vallan A, Parvis M, Galan M. Monitoring of the primary drying of a lyophilization process in vials. *Chem. Eng. Process.* 2009; 48(1):408–423.
83. Pikal MJ, Roy ML, Shah S. Mass and heat transfer in vial freeze-drying of pharmaceuticals: role of the vial. *J. Pharm. Sci.* 1984;73(9):1224–1237.
84. Rambhatla S, Pikal MJ. Heat and mass transfer scale-up issues during freeze-drying. I. Atypical radiation and the edge vial effect. *AAPS PharmSciTech* 2003;4(2):111–120.
85. Brülls M, Rasmuson A. Heat transfer in vial lyophilization. *Int. J. Pharm.* 2002;246(1–2):1–16.
86. Gan KH, Bruttini R, Crosser OK, Liapis AI. Freeze-drying of pharmaceuticals in vials on trays: effects of drying chamber wall temperature and tray side on lyophilization performance. *Int. J. Heat Mass Transf.* 2005;48(9):1675–1687.
87. Rambhatla S, Pikal MJ. Heat and mass transfer issues in freeze-drying process development. *Biotechnol. Pharm. Aspects* 2004;2:75–109.
88. Tsinontides SC, Rajniak P, Pham D, Hunke WA, Placek J, Reynolds SD. Freeze drying: principles and practice for successful scale-up to manufacturing. *Int. J. Pharm.* 2004;280 (1–2):1–16.
89. Tchessalov S, Dixon D, Nick W.Principles of lyophilization scale up. *Am. Pharm. Rev.* 2007; 10(3), 88–92.
90. Searles J. Observation and implications of sonic water vapor flow during freeze-drying. *Am. Pharm. Rev.* 2004;7(2):58, 60, 62, 64, 66–68, 75.
91. Rasetto VM, Daniele L, Baressi Antonello A.Computational fluid dynamics in freeze-drying technology. *Freeze Drying of pharmaceuticals and Biologicals*, Breckenridge, CO, 2008.
92. Patel SM, Chaudhuri S, Pikal MJ.Choked Flow and Importance of Mach I in Freeze-Drying Process Design. *Freeze Drying of Pharmaceutical and Biologicals,* Breckeridge, CO, 2008.
93. Alexeenko AA, Ganguly A, Nail SL. Computational analysis of fluid dynamics in pharmaceutical freeze-drying. *J. Pharm. Sci.* 2009;98(9):3483–3494.